Scaling laws of the dissipation rate of turbulent subgrid-scale kinetic energy

Charles Meneveau and John O'Neil
Department of Mechanical Engineering, The Johns Hopkins University, Baltimore, Maryland 21218
(Received 6 December 1993)

The energy dissipation term appearing in the transport equation for turbulent subgrid-scale kinetic energy k is studied experimentally. Special attention is directed at the scaling properties of its moments, which are described using the multifractal formalism. In large-eddy simulations, the dissipation is usually modeled in terms of k. Therefore, the scaling of moments of k is studied as well. It is found that the latter variable displays a slightly more pronounced level of intermittency than that of the dissipation, a discrepancy whose impact on simulations is difficult to assess *a priori*. However, it is shown that the scaling of the expected value of dissipation conditioned upon the local kinetic energy differs markedly from the model prediction. The equation for the probability density function is used to illustrate the importance of correctly predicting this conditional expected value. An alternative model is proposed that employs the inverse strain-rate magnitude as a time scale.

PACS number(s): 47.27.Gs

I. INTRODUCTION

The phenomenon of spatial and temporal intermittency of the small-scale structure of turbulence has attracted considerable attention over the last decades. The starting point has been a prediction based on the Kolmogorov [1] theory, for the longitudinal velocity structure function of order p, in (locally) isotropic turbulence:

$$\langle \Delta_r u^p \rangle \equiv \langle [u_1(\mathbf{x}+r\mathbf{e}_1)-u_1(\mathbf{x})]^p \rangle \sim c_p (\langle \epsilon \rangle r)^{\xi_p} , \qquad \xi_p = \frac{p}{3} . \tag{1}$$

Here ϵ is the rate of molecular dissipation of kinetic energy, as defined as

$$\epsilon = 2\nu S_{ij} S_{ij} , \tag{2}$$

where

$$S_{ij} \equiv \frac{1}{2}\left(\frac{\partial u_i}{\partial x_j} + \frac{\partial u_j}{\partial x_i} \right)$$

is the rate-of-strain tensor, ν is the kinematic viscosity, and $\mathbf{e}_1$ is a unit vector in the 1 direction. For $p=3$, and assuming (local) isotropy, Eq. (1) can be rigorously derived from the Navier-Stokes equations (yielding $c_3 = -\frac{4}{5}$). For other values of p, no analytical results are known to exist [2]. Experimentally, there is ample evidence (see, e.g., Ref. [3]) that the original prediction $\xi_p = p/3$ does not hold for large values of p. In addition, the dissipation rate was observed to be highly intermittent [4]. In view of such observations, the phenomenological grounding of Eq. (1) was expanded to relate the properties of $\langle \Delta_r u^p \rangle$ to those of the box-averaged dissipation ϵ_r [5,6]. The latter is defined as

$$\epsilon_r(\mathbf{x}) = \frac{1}{r^d} \int_{\Omega_r(\mathbf{x})} \epsilon(\mathbf{x}') d^d \mathbf{x}' , \tag{3}$$

where $\Omega_r(\mathbf{x})$ is a d-dimensional cube (a linear segment in most experimental measurements) of size r, centered at $\mathbf{x}$. The suspected relationship between the two variables reads as follows:

$$\langle \Delta_r u^p \rangle \sim c_p \langle (\epsilon_r r)^{p/3} \rangle . \tag{4}$$

A considerable amount of evidence supporting this relation has accumulated (compare results of Refs. [3,7–10, etc.]). Other studies have focused directly on statistics of $\Delta_r u$ conditioned on local values of ϵ_r. This issue is inspired by Kolmogorov's refined similarity hypothesis [5] (also Obukhov [6]), which implies that the conditional expected value scales as

$$\langle |\Delta_r u| \, | \epsilon_r \rangle \sim (r\epsilon_r)^{1/3} . \tag{5}$$

The latter expression has recently received a considerable amount of experimental [11–13] as well as computational [14] support.

Traditionally, the variable $\epsilon_r(\mathbf{x})$ is interpreted, rather loosely, as a surrogate for the spectral energy flux that occurs at scale r and location $\mathbf{x}$. The underlying question that is being posed, implicitly or explicitly, is the following: "Given the spectral flux of energy, how do other variables of the inertial range (such as velocity differences) behave?" In reality, by using ϵ_r as a surrogate for the energy flux, the question that has been addressed is "given the flux at dissipation-range scales, what is the behavior of the inertial-range variables?"

The purpose of the present paper is to revisit these fundamental questions from the point of view of modeling for the large-eddy-simulation (LES) of turbulence. The underlying aim is to interpret relationships such as Eq. (4) as closures for small-scale variables. However, the question of practical relevance will be shown to be reserved from that reviewed above, i.e., we will have to ask "given a variable in the inertial range, how do the dissipative-range variables behave?" As will be shown in Sec. II, the dissipation-range quantity of interest in the

context of LES differs slightly from ϵ_r. This serves as motivation to reexamine the scaling properties of this new variable using experimental data, which is done in Sec. IV. Also, the dissipation results are compared to the scaling properties of the subgrid-kinetic energy, which is commonly used as a model for the dissipation term. Kolmogorov's refined similarity hypothesis is then revised in Sec. V from the point of view of modeling for LES. Concluding remarks are presented in Sec. VI.

II. DYNAMICS OF SUBGRID-SCALE KINETIC ENERGY

Filtering of the Navier-Stokes (NS) equation for an incompressible fluid gives rise to the LES equations

$$\frac{\partial \bar{u}_i}{\partial x_i}=0 , \tag{6}$$

$$\frac{\partial \bar{u}_i}{\partial t}+\bar{u}_j\frac{\partial \bar{u}_i}{\partial x_j}=-\frac{\partial}{\partial x_j}\left[\frac{\bar{p}}{\rho}\delta_{ij}+\tau_{ij}\right]+\nu\nabla^2\bar{u}_i , \tag{7}$$

where an overbar represents a field convolved with a spatial filter of characteristic width Δ (or some anisotropic filter with widths Δ_i in each direction, $i=1,2,3$). The subgrid-scale (SGS) stress tensor τ_{ij} is defined as

$$\tau_{ij}\equiv\overline{u_i u_j}-\bar{u}_i\bar{u}_j . \tag{8}$$

In order to numerically solve Eq. (7) on a computational mesh with a grid size of order Δ, one needs a SGS model for $\tau_{ij}(\mathbf{x},t)$ (for a review of LES, see, e.g., Ref. [15]). The most common approach is to postulate, for the deviatoric part of τ_{ij}, an eddy-viscosity closure, in which the eddy viscosity ν_T is computed based on the local magnitude of the resolved rate-of-strain tensor $\bar{S}_{ij}$ (the Smagorinsky model):

$$\tau_{ij}^{\text{dev}}=-2\nu_T\bar{S}_{ij} , \quad \nu_T=(c_S\Delta)^2|\bar{S}| . \tag{9}$$

However, when the turbulence is highly unsteady, it has been recognized that some dependence on a fluid element's past history should be taken into consideration. This can be accomplished [16,17] by expressing the eddy viscosity in terms of the subgrid-kinetic energy k_Δ,

$$\nu_T=c_k\Delta\sqrt{k_\Delta} , \tag{10}$$

where

$$k_\Delta\equiv\tfrac{1}{2}(\overline{u_p u_p}-\bar{u}_p\bar{u}_p) ,$$

and writing an additional transport equation for this new variable (k_Δ) [18]. The transport equation for k_Δ is obtained by multiplying the NS equations by u_p, filtering, and subtracting the LES equations multiplied by $\bar{u}_p$ (see, e.g., Ref. [19]). It reads

$$\frac{\partial \bar{k}_\Delta}{\partial t}+\bar{u}_j\frac{\partial \bar{k}_\Delta}{\partial x_j}=\mathcal{P}-\mathcal{E}_\Delta-\frac{\partial Q_j}{\partial x_j} . \tag{11}$$

Here

$$\mathcal{P}=-\tau_{ij}\bar{S}_{ij} \tag{12}$$

represents the production of SGS kinetic energy, and can be self-consistently expressed using the closure for τ_{ij}. The vector Q_i represents flux of k_Δ due to turbulence and viscous action, and does not occupy our interest here. It is itself usually modeled using an eddy-viscosity Ansatz. Arguably, the biggest challenge for modeling in Eq. (11) comes from the term $\mathcal{E}_\Delta$, which represents the dissipation of k due to molecular viscosity. It is defined as follows:

$$\mathcal{E}_\Delta=2\nu(\overline{\bar{S}_{pq}\bar{S}_{pq}}-\bar{S}_{pq}\bar{S}_{pq}) . \tag{13}$$

As opposed to all other terms in Eq. (11), it is dominated by the smallest of the unresolved length scales of turbulence. Comparison of Eqs. (3) and (13) illustrates the fact that if the overbar filtering is interpreted as a box filter in physical space, then $\mathcal{E}_\Delta$ equals ϵ_Δ except for an additive term $2\nu\bar{S}_{pq}\bar{S}_{pq}$. As outlined in Sec. I, much empirical data exists regarding ϵ_Δ. However, not much is known about $\mathcal{E}_\Delta$, a state of affairs not quite satisfactory given the direct practical relevance of $\mathcal{E}_\Delta$ for the simulation of turbulent flow. One of the questions we wish to address (Sec. IV) is whether $\mathcal{E}_\Delta$ displays the same statistical and scaling features as ϵ_Δ. Although standard, high Reynolds number, scaling arguments suggest that the second term on the right-hand side (rhs) of Eq. (13) must be small compared to the first, the question is worth answering based on real data. The study of scaling features is performed here using the standard multifractal formalism [20–22, 7], in which moments of $\mathcal{E}_\Delta$ are characterized by their scaling exponents with respect to the filter width:

$$\frac{\langle \mathcal{E}_\Delta^q\rangle}{\langle \mathcal{E}_\Delta\rangle^q}\sim\left[\frac{\Delta}{L}\right]^{(q-1)(D_q^{\mathcal{E}}-d)} . \tag{14}$$

Here $D_q^{\mathcal{E}}$ is the set of generalized dimensions of the dissipation field. Once $D_q^{\mathcal{E}}$ is known, one can also obtain the spectrum of singularities $f(\alpha)$ of this intermittent field, by Legendre transformation [21,22].

Returning to Eq. (11), the strategy typically employed to model the dissipation term is to replace $\mathcal{E}_\Delta$ by $\mathcal{E}_\Delta^*$, where

$$\epsilon_\Delta^*=c_{\mathcal{E}}\frac{k_\Delta^{3/2}}{\Delta} . \tag{15}$$

Therefore, another question that needs to be addressed is to what degree does $\mathcal{E}_\Delta^*$ display properties that are similar to those of $\mathcal{E}_\Delta$ or ϵ_Δ. Arguably, the more features they display in common, the better are the chances that the modeling embodied in Eq. (15) can yield realistic time evolutions of the SGS kinetic energy, once the LES equations are integrated. Thus, in Sec. IV, a study of the multifractal properties of $\mathcal{E}_\Delta^*$ is undertaken.

While the comparison of intermittency characteristics of real and modeled rates of dissipation will provide some insight about the goodness of a model, it is difficult to ascertain what effect an eventual agreement (or disagreement) of $\mathcal{E}$ statistics would have on an actual LES. On the other hand, some progress can be made by attempting to find necessary conditions that the model must obey in order to produce correct flow statistics during LES [23].

In the present context, let us inquire about necessary conditions on the model for $\mathcal{E}_\Delta$ so that the LES produce the correct joint (single-point) probability-density function of resolved velocity *and* SGS kinetic energy. This joint PDF is denoted by $f(K,\mathbf{V};\mathbf{x},t)$, where K is the argument corresponding to the SGS kinetic energy (a realization is denoted by k_Δ) and $\mathbf{V}$ is the argument corresponding to resolved velocity (whose realization is, as before, denoted by $\bar{\mathbf{u}}$). The transport equation that is obeyed by the joint PDF can be deduced by standard methods [24,25] applied to the LES equations [23],

$$\frac{\partial f}{\partial t}+V_j\frac{\partial f}{\partial x_j}=-\frac{\partial}{\partial V_j}[f\langle A_j|K,\mathbf{V}\rangle] -\frac{\partial}{\partial K}[f\langle \mathcal{P}-\nabla\cdot\mathbf{Q}|K,\mathbf{V}\rangle] +\frac{\partial}{\partial K}[f\langle \mathcal{E}_\Delta|K,\mathbf{V}\rangle]\ . \tag{16}$$

Here A_j is the (filtered) force per unit mass, i.e., the entire right-hand side of Eq. (7). The above equation is to be understood as representing the joint statistics resulting from an ensemble of realizations of a real turbulent flow. As in Ref. [23], one can write a similar equation for the joint statistics that would result from a LES. There, the last term would involve the model expression for $\mathcal{E}_\Delta$, instead of the real dissipation. Clearly, in order for the LES to reproduce the correct joint PDF *and* the other terms appearing on the rhs of Eq. (16), *at least* the equality

$$\langle \mathcal{E}_\Delta|K,\mathbf{V}\rangle=\langle \mathcal{E}_\Delta^*|K,\mathbf{V}\rangle \tag{17}$$

must hold (up to a constant with respect to k_Δ). The above expression is thus a necessary condition. Similar arguments have been made in Ref. [23], in more detail but in a different context. It follows that the average rate of dissipation conditioned only on k_Δ,

$$\langle \mathcal{E}_\Delta|k_\Delta\rangle=\int\langle \mathcal{E}_\Delta|k_\Delta,\mathbf{V}\rangle f(\mathbf{V})d^3\mathbf{V}\ , \tag{18}$$

must be predicted properly (for notational simplicity we now employ k_Δ for both the argument of the conditional average and for the realization). If $\langle \mathcal{E}_\Delta|k_\Delta\rangle$ is not predicted correctly, the joint conditional average cannot be correct in all values of its arguments.

In summary, if

$$\langle \mathcal{E}_\Delta|k_\Delta\rangle\neq\langle \mathcal{E}_\Delta^*|k_\Delta\rangle \tag{19}$$

then we can state unambiguously that it is not possible for the LES to simultaneously reproduce the correct joint PDF of $(\bar{\mathbf{u}},k_\Delta)$ and the terms on the rhs of Eq. (16). Thus the conditional expectation $\langle \mathcal{E}_\Delta|k_\Delta\rangle$ is seen to have special relevance to LES. It is interesting to notice that the conditioning is reversed from that of the studies to date on Kolmogorov's refined similarity hypothesis: Here we are given an inertial-range variable (k_Δ) and inquire about the small-scale variable $\mathcal{E}_\Delta$.

The prediction of the model of Eq. (15) is simple:

$$\langle \mathcal{E}_\Delta^*|k\rangle=\frac{c_\mathcal{E}}{\Delta}\langle k^{3/2}|k\rangle=\frac{c_\mathcal{E}}{\Delta}k^{3/2}\ . \tag{20}$$

It is thus of interest to perform measurements of the real conditional average and compare with this prediction. This task will be described in Sec. V.

III. EXPERIMENTAL DATA

Two sets of experimental data were employed for this study. The first consists of measurements obtained in the wake of a circular cylinder. Details of the experimental set up and instrumentation are given in Ref. [26]. The measurements were taken on centerline, at 100 diameters downstream of the 5-cm-diam cylinder. The measurements consist of a temporal record of the fluctuating streamwise velocity component, obtained with a subminiature hot-wire sensor. The mean velocity was 27.3 m/s , the (longitudinal) integral scale was $L_1=0.19$ m, and the Kolmogorov scale (estimated from usual isotropy assumption) was $\eta=0.13$ mm. The Taylor scale Reynolds number was $\mathrm{Re}_\lambda\sim480$. As shown in Ref. [26], the resulting energy spectrum displays a considerable inertial range with a $-\frac{5}{3}$ slope, and collapses well with the universal curve, including much of the decay in the dissipation range. A total of 1.3×10^5 data points are used for the present analysis, representing a total length corresponding to about 3.0×10^2 integral scales. The second set of data corresponds to single hot-wire measurements in the atmospheric surface layer (at a height of $L=18$ m), performed at Yale University. The data set is the same as that documented and analyzed in Ref. [7]. The microscale Reynolds number is estimated as $\mathrm{Re}_\lambda\sim1500$. However, only a limited record length (corresponding to $\sim18L$) is available. As discussed in Ref. [26], this precludes acceptable convergence of high-order moments. However, the data will be employed to illustrate trends when they are robust with respect to record length, i.e, for the conditional averages. We employ Taylor's frozen flow hypothesis and interpret the time record as a linear spatial cut through the flow. This is an acceptable practice, since the relative turbulence intensity is low.

Data processing

As outlined in the last section, our goal here is to study the scaling of moments of the dissipation rate $\mathcal{E}_\Delta$. As is traditionally done, a one-dimensional surrogate of $\mathcal{E}_\Delta$ is constructed based on the experimental hot-wire data. Also, we immediately normalize the variables with their ensemble average. Thus, we compute

$$\left.\frac{\mathcal{E}_\Delta}{\langle\mathcal{E}_\Delta\rangle}\right|_{d=1}=\frac{\overline{\left[\frac{\partial u_1}{\partial x_1}\right]^2}-\left[\frac{\partial\bar{u}_1}{\partial x_1}\right]^2}{\left\langle\overline{\left[\frac{\partial u_1}{\partial x_1}\right]^2}-\left[\frac{\partial\bar{u}_1}{\partial x_1}\right]^2\right\rangle}\ . \tag{21}$$

The filtering overbar denotes linear filtering of the one-dimensional (1D) data record, with a filter size Δ. Two types of filters were considered, with no appreciable difference in results: the Gaussian filter

$$F_\Delta(x)=\frac{1}{\Delta}\left[\frac{6}{\pi}\right]^{1/2}e^{-6(x/\Delta)^2}\ , \tag{22}$$

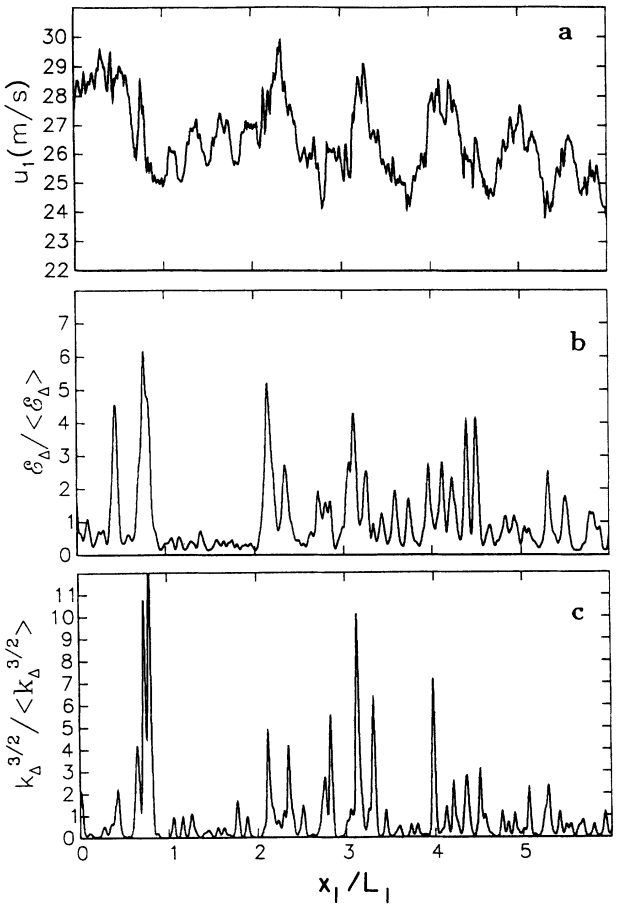

FIG. 1. (a) Measured time trace of the streamwise velocity u_1. The time trace is interpreted here as a spatial signal along the x_1 axis using Taylor's hypothesis. (b) Measured one-dimensional surrogate of the rate of dissipation of turbulent kinetic energy. The signal is normalized by its mean value. (c) Measured signal of the $\frac{3}{2}$ power of the subgrid-scale kinetic energy. The filter width was $\Delta = L_1/15$, where L_1 is the longitudinal integral scale.

and the top-hat filter

$$F_\Delta(x) = \frac{1}{\Delta}\ , \quad \text{if } |x| < \frac{\Delta}{2}\ , \text{ and zero otherwise .} \tag{23}$$

The derivatives are computed using finite differences from consecutive samples of velocities.

Figure 1 shows a segment of the velocity signal (a) of length corresponding to six integral scales L_1 (~ 20 cylinder diameters $\sim 5.0\times 10^3\eta$). In 1(b) the normalized dissipation rate computed according to Eq. (21) is shown. The filter size for this signal is $\Delta = L_1/15$, and the Gaussian filter was used. The signal displays a high level of intermittency, which we have observed to strongly increase with decreasing filter size. In 1(c), we show the local kinetic energy k, also to be discussed in Sec. IV.

IV. SCALING PROPERTIES OF $\mathcal{E}_\Delta$ and $\mathcal{E}_\Delta^*$

The moments of the dissipation

$$\left\langle \left[\frac{\mathcal{E}_\Delta}{\langle \mathcal{E}_\Delta \rangle} \right]^q \right\rangle$$

are computed for a range of values of Δ and of q. These moments are plotted in Fig. 2 for the wake flow, in such a fashion that the slope corresponds to $D_q^{\mathcal{E}}$. This slope is obtained by (least-squares) linear regression, in log-log units. The range over which the fit is taken (shown by the solid lines) corresponds to standard estimates of the location of the inertial range; $\Delta > 30\eta$ and, here, up to $\Delta \sim L_1/3$. For negative q, the range is restricted to $\Delta > 60\eta$. The resulting $D_q^{\mathcal{E}}$ curve is shown in Fig. 3 (solid line). The error bars represent the change in slope if the fit is performed in different ranges (between $15 < \Delta/\eta < 300$ and $100 < \Delta/\eta < 2000$). Thus the error bars give some qualitative indication of the sensitivity of the exponents on the choice of scaling range. The corresponding singularity spectrum is obtained through the standard Legendre transform [22,7], and is shown in Fig. 4. The symbols represent the average curve through previous results [27], obtained from the standard dissipation

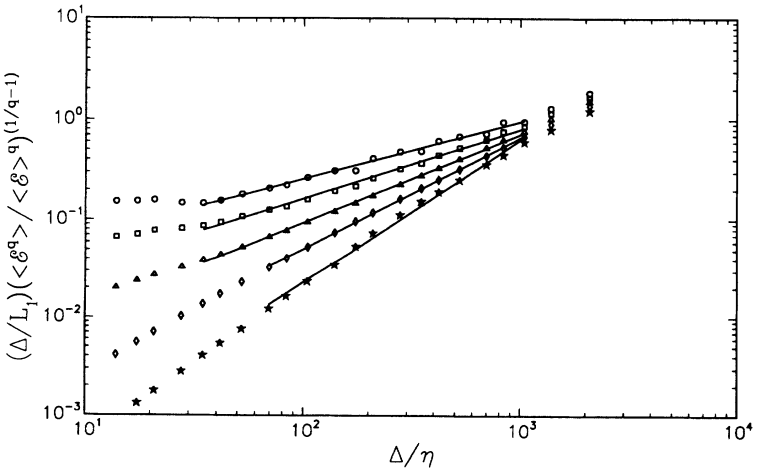

FIG. 2. Log-log plot of qth-order moments of dissipation of SGS kinetic energy as a function of filter width, obtained in the wake flow. The results are plotted so that the slope corresponds to $D_q^{\mathcal{E}}$. Different symbols are for different values of q (circles: $q=4$; squares: $q=2.4$; triangles: $q=0.8$; diamonds: $q=-0.8$; stars: $q=-2.4$). The solid line shows the least-squares error fit in the inertial range.

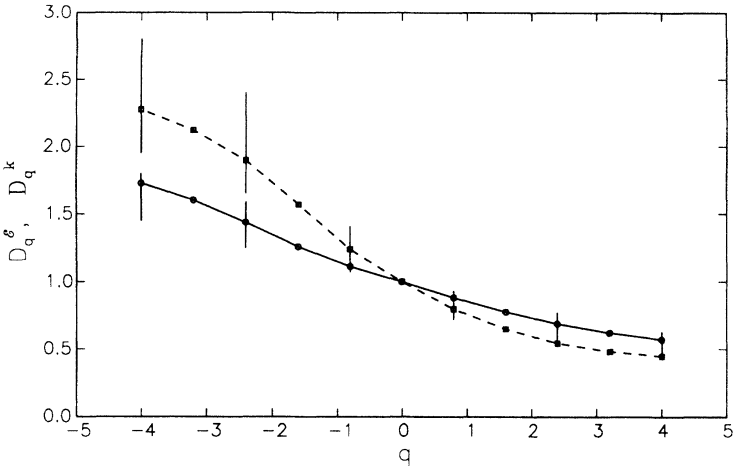

FIG. 3. Solid line: Moment exponents of $\mathcal{E}_\Delta$, the (1D surrogate of) dissipation of SGS kinetic energy, for the wake flow. Dashed line: moment exponents of $k_\Delta^{3/2}$, the (1D surrogate of) model for dissipation of SGS kinetic energy, for the wake flow. Error bars give some indication associated with the selection of the scaling range.

variable ϵ_r rather than $\mathcal{E}$. No significant difference is seen between the two variables, except in the low-intensity region. There the experimental uncertainty is quite large however. The overall agreement between the scaling properties of $\mathcal{E}_\Delta$ and ϵ_Δ is not entirely surprising, given the fact that the difference between the two (representing the viscous dissipation of the large scales) is quite small.

Next we examine the scaling properties of the model for dissipation based on SGS kinetic energy. For this purpose, we require a one-dimensional surrogate of k_Δ. We approximate it in terms of the streamwise velocity component. Also, since it is really the $\frac{3}{2}$ power of k we are interested in, we compute the following quantity:

$$\left.\frac{\mathcal{E}_\Delta^*}{\langle \mathcal{E}_\Delta^* \rangle}\right|_{d=1} = \frac{\overline{u_1^2}-(\bar{u}_1)^2}{\langle \overline{u_1^2}-(\bar{u}_1)^2 \rangle} . \tag{24}$$

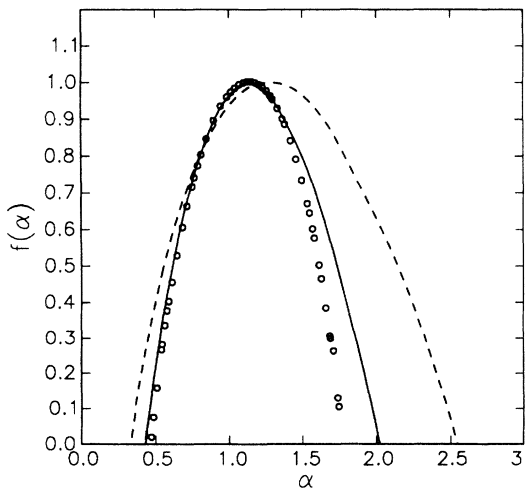

FIG. 4. Solid line: singularity spectrum of $\mathcal{E}_\Delta$ obtained from Legendre transformation of the previous curves. The dashed line shows the results corresponding to the modeled dissipation $k_\Delta^{3/2}$. The symbols are the average results corresponding to the standard definition of dissipation ϵ_r, as reported in Ref. [5].

Figure 1(c) shows a segment of this variable. Comparison with 1(b) suggests that the two variables display some degree of correlation, while $\mathcal{E}_\Delta$ is slightly more intermittent. We recall that in a LES, the relevance of $\mathcal{E}_\Delta^* = c_\epsilon k_\Delta^{3/2}/\Delta$ is that it serves as a model for $\mathcal{E}_\Delta$. Of direct interest in this context is the correlation coefficient between the two variables. It is computed based on the data in the wake and atmospheric surface layer and is displayed in Fig. 5, as a function of filter width Δ. As can be seen, there is a level of correlation of about $\rho \sim 0.6$. It is noteworthy that this correlation is significantly higher than what is typically observed when comparing real and modeled subgrid stresses using the eddy-viscosity models [23].

Next, the q moments of the expression in Eq. (24) are computed. The procedure is exactly as in the last section, and the resulting log-log plots are shown in Fig. 6 for the wake flow. The slopes are obtained in the same fashion as explained in the last section, and are depicted in Fig. 3 with the dashed line. After Legendre transforming the results, the singularity spectra are obtained, which is shown in Fig. 4 as the dashed line. At the left side of the curve (representing the scaling of high-intensity points of the signals) a small difference between the results is observed. It implies that $k_\Delta^{3/2}$ is slightly more intermittent than $\mathcal{E}_\Delta$. This is consistent with our earlier qualitative observations based on the signals themselves. On the other hand, the low-intensity regions display some difference in their scaling behavior, arguably outside experimental uncertainty. Again, $k_\Delta^{3/2}$ is more "patchy," in the following sense. Regions where $k_\Delta^{3/2}$ is very close to zero (large α's) are more prevalent than those where $\mathcal{E}_\Delta$ is very close to zero.

V. CONDITIONAL AVERAGES

In this section, we study the conditional expected values

$$\langle k_\Delta | \mathcal{E}_\Delta \rangle \quad \text{and} \quad \langle \mathcal{E}_\Delta | k_\Delta \rangle .$$

The first is very similar to the variable studied in recent studies of Kolmogorov's refined similarity hypothesis. Its

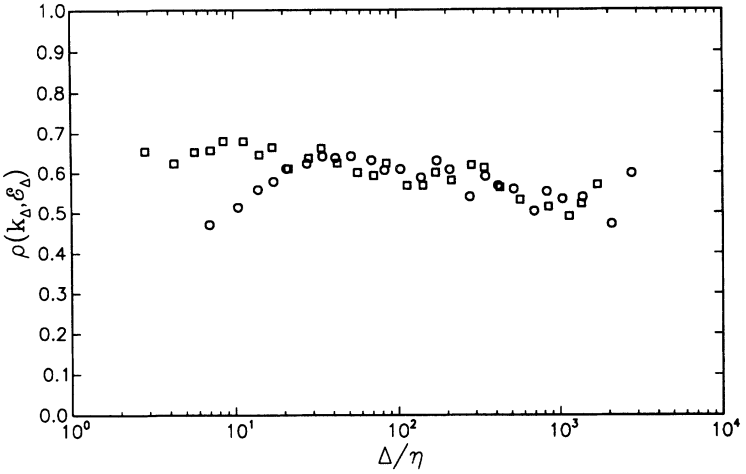

FIG. 5. Measured correlation coefficient between local dissipation $\mathcal{E}_\Delta$ and local kinetic energy k_Δ, as a function of filter width Δ. Results are shown for the wake flow (circles) and atmospheric flow (squares).

expected scaling (neglecting small intermittency corrections), based on the refined similarity hypothesis, is

$$\langle k_\Delta | \mathcal{E}_\Delta \rangle \sim \Delta^{2/3} \mathcal{E}_\Delta^{2/3} . \tag{25}$$

We have computed this conditional average from the data, for both the wake flow and the atmospheric flow. The results are shown in Figs. 7 and 8, respectively. For reference, the dotted line has a slope equal to $\frac{2}{3}$. As can be seen, the scaling implied by the refined similarity hypothesis is corroborated very well by the present data. This conclusion is valid for a large range of Δ values. These results are also consistent with recent findings of [11–14], with the difference that we now corroborated the hypothesis for the variables of present interest, k_Δ and $\mathcal{E}_\Delta$.

However, as outlined in Sec. II, the quantity that is of direct relevance in the context of LES modeling of the SGS kinetic-energy equation is the second (reversed) expected value $\langle \mathcal{E}_\Delta | k_\Delta \rangle$. When this quantity is computed from our data, the plots in Figs. 9 and 10 are obtained, for the wake and atmospheric flows, respectively. The scaling $\langle \mathcal{E}_\Delta | k_\Delta \rangle \sim k_\Delta^{3/2}$, which is expected both from the (reversed) refined hypothesis and from the model discussed before, is displayed by the dotted lines (with slope $\frac{3}{2}$) in Figs. 9 and 10. As is quite clear, the data are not consistent with this scaling. The observation is made for all filter sizes, for the two filter types considered and for both flows at widely different Reynolds numbers. The observed trend means that the rate of dissipation depends more weakly on the kinetic energy than assumed by the refined similarity hypothesis and/or by the modeling in terms of $k_\Delta^{3/2}$. Some dependence of the slope on Δ is seen for the wake flow. Since the dependence is much weaker for the atmospheric flow, it is possible that it is a Reynolds number effect.

VI. CONCLUSIONS

An experimental study of scaling of small-scale variables in turbulent flows has been performed. Instead of focusing on traditional variables such as structure functions, box-averaged rates of dissipation, and conditional averages of velocity increments, we have examined similar variables which have more direct applicability to modeling of turbulent flow through large-eddy simulation. It was found that the rate of dissipation appearing in the LES transport equation was very similar to the traditional box-averaged dissipation, ϵ_r. Among others, this observation endows previous studies on ϵ_r with in-

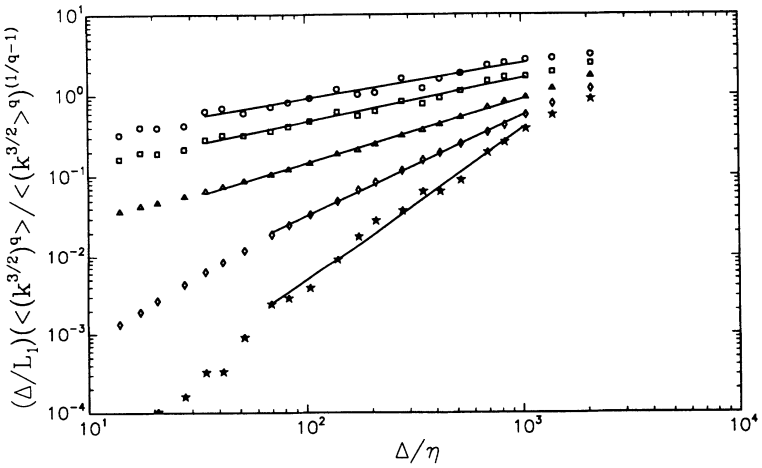

FIG. 6. Log-log plot of qth-order moments of SGS kinetic energy (to the $\frac{3}{2}$ power) as a function of filter width, obtained in the wake flow. The results are plotted so that the slope corresponds to D_q^k. Different symbols are for different values of q (circles: $q=4$; squares: $q=2.4$; triangles: $q=0.8$; diamonds: $q=-0.8$; stars: $q=-2.4$). The solid line shows the least-squares error fit in the inertial range.

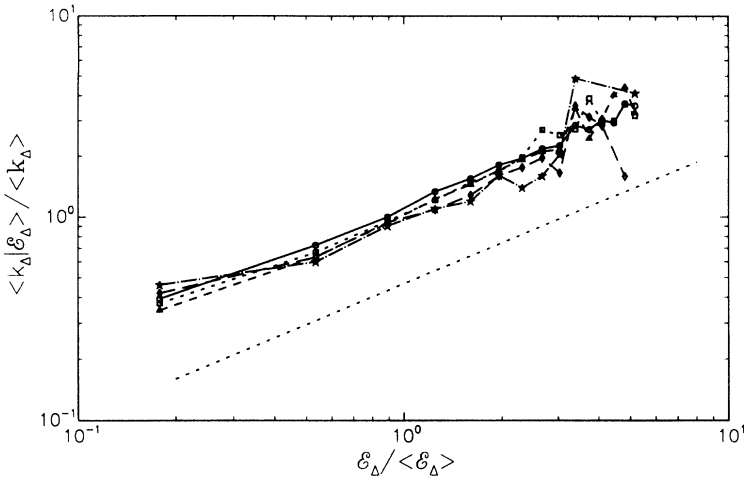

FIG. 7. Conditional expected value of the SGS kinetic energy, measured in the wake flow using the 1D surrogate variables. The conditioning is done as a function of the local value of the dissipation rate $\mathcal{E}_\Delta$. Different symbols correspond to different filter sizes (circles: $\Delta/\eta=20$; squares: $\Delta/\eta=50$; open triangles: $\Delta/\eta=130$; diamonds: $\Delta/\eta=330$; stars: $\Delta/\eta=800$). The dotted line has a slope of $\frac{2}{3}$ and represents the scaling implied by the Kolmogorov refined similarity hypothesis.

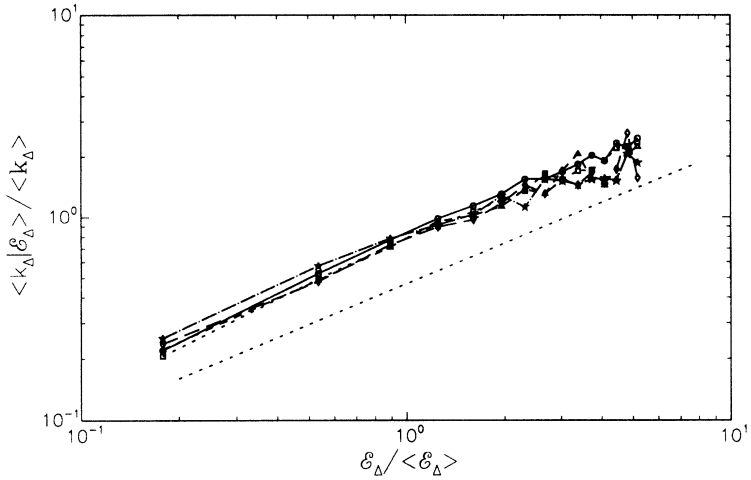

FIG. 8. Conditional expected value of the SGS kinetic energy, measured in the atmospheric surface layer. Different symbols correspond to different filter sizes (circles: $\Delta/\eta=9$; squares: $\Delta/\eta=23$; open triangles: $\Delta/\eta=60$; diamonds: $\Delta/\eta=140$; stars: $\Delta/\eta=360$). The dotted line has a slope of $\frac{2}{3}$.

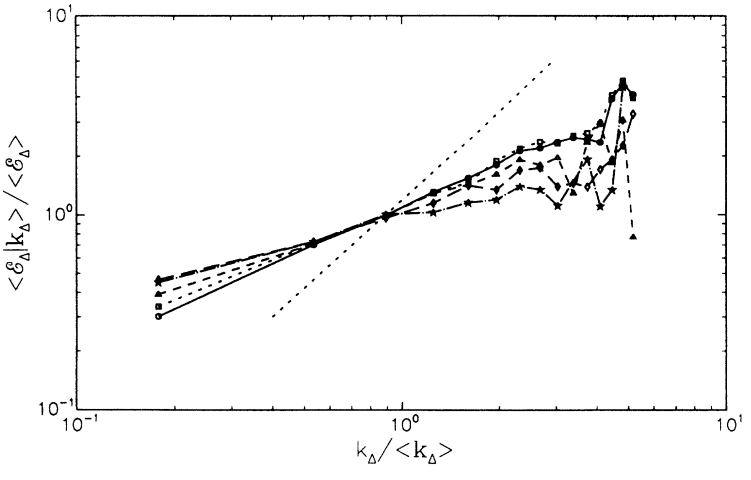

FIG. 9. Conditional expected value of the rate of dissipation of SGS kinetic energy $\mathcal{E}_\Delta$, measured in the wake flow using the 1D surrogate variables. The conditioning is done as a function of the local value of the SGS kinetic energy k_Δ. Results for different filter sizes are denoted by the same symbols as in Fig. 7. The dotted line has a slope of $\frac{3}{2}$.

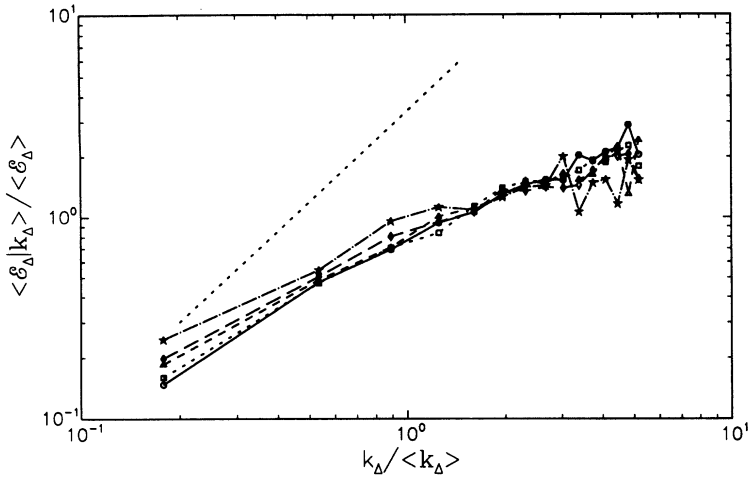

FIG. 10. Conditional expected value of the rate of dissipation of SGS kinetic energy $\mathcal{E}_\Delta$, measured in the atmospheric surface layer. Results for different filter sizes are denoted by the same symbols as in Fig. 8.

creased practical relevance.

A comparison was then made between the scaling properties of the dissipation rate and an expression based on the SGS kinetic energy k_Δ. This expression has been employed to model the dissipation term, which is not known during LES. The comparison was made in terms of their multifractal spectra [both variables are (quasi) "singular" measures]. It was found that they displayed a correlation which is higher than that observed for the eddy-viscosity closure at the level of the stress tensor. The degree of intermittency of $k_\Delta^{3/2}$ was shown to be higher than that of the dissipation, but by a small amount. It is not clear how this discrepancy would influence the outcome of a LES.

The transport equation for the SGS kinetic energy was employed to derive an equation for the joint PDF of k_Δ and resolved velocity. One of the terms appearing in that equation is the average rate of dissipation, conditioned on SGS kinetic energy and the resolved velocity vector. It was shown that in order for the LES to properly reproduce all statistics at this joint PDF level, the correct prediction of the expected value $\langle \mathcal{E}_\Delta | k_\Delta \rangle$ is a necessary condition. However, the measurements displayed a scaling $\langle \mathcal{E}_\Delta | k_\Delta \rangle \sim k_\Delta^\beta$ more in line with $\beta \sim 1$ (or even lower) than with a value of $\beta = \frac{3}{2}$. This unexpected scaling means that LES employing $k^{3/2}/\Delta$ as a model for the dissipation will produce errors in some statistics at the joint PDF level [either in the joint PDF itself, and/or in the other conditional expectations appearing in Eq. (16)]. As a check of consistency of our data with previous work, we found that it displays the expected scaling of the reversed conditional expectation, $\langle k_\Delta | \mathcal{E}_\Delta \rangle \sim \mathcal{E}_\Delta^{2/3}$.

We now point out a possible remedy for the modeling. Clearly, on dimensional grounds the value $\beta = \frac{3}{2}$ is a necessity if we want to express $\mathcal{E}_\Delta$ only in terms of the local value of the kinetic energy and the filter width. Another (local) variable on which $\mathcal{E}_\Delta$ could depend is the resolved strain-rate magnitude $|\bar{S}|$. Dimensionally, one could thus write

$$\mathcal{E}_\Delta^* \sim c \frac{k_\Delta^\beta |\bar{S}|^{3-2\beta}}{\Delta^{2(\beta-1)}} . \tag{26}$$

It is recognized that for $\beta = \frac{1}{2}$, the dissipation term would exactly mirror the scaling of the production of SGS kinetic energy $-\tau_{ij}\bar{S}_{ij}$, once the eddy-viscosity expression (9) is employed for the stress. Since in an equilibrium condition the two should display the same mean value, by setting $\beta = \frac{1}{2}$ the two terms would cancel each other out exactly. This is not a desirable feature for a model. The choice $\beta = 1$, on the other hand, appears to be worthwhile to explore. Therefore a possible model is $\mathcal{E}_\Delta^* \sim c k_\Delta |\bar{S}|$, whose physical interpretation is simply that the time scale is now computed based on the resolved strain rate ($\sim |\bar{S}|^{-1}$) and not based on the SGS kinetic energy (Δ / k_Δ).

If k_Δ and $|\bar{S}|$ were statistically independent, then the conditional average $\langle k_\Delta |\bar{S}|\, | k_\Delta \rangle$ would scale as k_Δ. However, based on our experimental data and on the assumption that $|\bar{S}| \approx |\partial \bar{u}_1 / \partial x_1|$, we find that $|\bar{S}|$ and k_Δ are quite correlated. As a consequence, the conditional average $\langle k_\Delta |\bar{S}|\, | k_\Delta \rangle$ scales approximately (again) as $\sim k_\Delta^{1.5}$ and not as $\sim k_\Delta^1$. One could, on the other hand, obtain the time scale at a larger scale according to $|\hat{S}|$ (where the circumflex denotes a filter of width, say, 4Δ or 8Δ). The correlation between k_Δ and $|\hat{S}|$ is small, and we find that the scaling exponent of $\langle k_\Delta |\hat{S}|\, | k_\Delta \rangle$ with k_Δ approaches 1. Thus a proposed model for the dissipation is $\mathcal{E}_\Delta^* \sim c k_\Delta |\hat{S}|$, where the strain rate is filtered at a scale $m\Delta$ ($m \geq 4$).

In terms of future studies, it would be of interest to check present results using 3D (or 2D) filtering instead of 1D filtering employed here. There could be differences in scaling due to the dimensionality of the filtering (see, e.g., Ref. [28]). This goal could be achieved by analyzing results of direct numerical simulations (3D), or by analyzing experimental results obtained from particle displacement velocimetry (2D) [29].

ACKNOWLEDGMENT

This work was performed with the financial support of the National Science Foundation, Grant No. CTS-9113048.

[1] A. N. Kolmogorov, C.R. Acad. Sci. U.S.S.R. **30**, 301 (1941).
[2] M. Nelkin, J. Stat. Phys. **54**, 1 (1989).
[3] F. Anselmet, Y. Gagne, E. J. Hopfinger, and R. A. Antonia, J. Fluid Mech. **140**, 63 (1984).
[4] G. K. Batchelor and A. A. Townsend, Proc. R. Soc. London Ser. A **199**, 238 (1949).
[5] A. N. Kolmogorov, J. Fluid Mech. **62**, 82 (1962).
[6] A. M. Obukhov, J. Fluid Mech. **62**, 77 (1962).
[7] C. Meneveau and K. R. Sreenivasan, J. Fluid Mech. **224**, 429 (1991).
[8] J. F. Muzy, E. Bacry, and A. Arneodo, Phys. Rev. Lett. **67**, 3515 (1992).
[9] I. Hosokawa and K. Yamamoto, Phys. Fluids A **2**, 889 (1990).
[10] A. Vincent and A. Meneguzzi, J. Fluid Mech. **225**, 1 (1991).
[11] G. Stolovitzky, P. Kailasnath, and K. R. Sreenivasan, Phys. Rev. Lett. **69**, 1178 (1992).
[12] S. T. Thoroddsen and C. W. Van Atta, Phys. Fluids A **4**, 2592 (1992).
[13] A. A. Praskovsky, Phys. Fluids A **4**, 2589 (1992).
[14] S. Chen, G. Doolen, R. H. Kraichnan, and Z-S She, Phys. Fluids A **5**, 458 (1993).
[15] W. C. Reynolds, in *Whither Turbulence? or Turbulence at Crossroads*, edited by J. L. Lumley (Springer, New York, 1990), p. 313.
[16] S. Ghosal, T. S. Lund, and P. Moin, in Center for Turbulence Research Annual Research Briefs, Stanford University (1992), (unpublished), p. 3.
[17] V. C. Wong, Phys. Fluids A **4**, 1081 (1992).
[18] J. W. Deardorff, Bound. Layer Meteor. **7**, 81 (1974).
[19] M. Germano, J. Fluid Mech. **238**, 325 (1992).
[20] B. B. Mandelbrot, J. Fluid Mech. **62**, 331 (1974).
[21] U. Frisch and G. Parisi, in *Turbulence and Predictability in Geophysical Fluid Dynamics and Climate Dynamics* (North-Holland, New York, 1985), p. 84.
[22] T. C. Halsey, M. H. Jensen, L. P. Kadanoff, I. Procaccia, and B. I. Shraiman, Phys. Rev. A **33**, 1141 (1986).
[23] C. Meneveau, Phys. Fluids **6**, 815 (1994).
[24] T. S. Lundgren, Phys. Fluids **10**, 969 (1967).
[25] S. B. Pope, Prog. Energy Combust. Sci. **11**, 119 (1985).
[26] J. O'Neil and C. Meneveau, Phys. Fluids A **5**, 158 (1993).
[27] C. Meneveau and K. R. Sreenivasan, Phys. Rev. Lett. **59**, 1424 (1987).
[28] A. Scotti, C. Meneveau, and D. K. Lilly, Phys. Fluids A **5**, 2306 (1993).
[29] S. Liu, C. Meneveau, and J. Katz, J. Fluid Mech. (to be published).